

C. GRIVAS^{1,✉}
T.C. MAY-SMITH¹
D.P. SHEPHERD¹
R.W. EASON¹
M. POLLNAU²
M. JELINEK³

Broadband single-transverse-mode fluorescence sources based on ribs fabricated in pulsed laser deposited Ti:sapphire waveguides

¹ Optoelectronics Research Centre (O.R.C.), University of Southampton, Highfield, Southampton SO17 1BJ, UK

² Institute of Imaging and Applied Optics, Swiss Federal Institute of Technology, 1015 Lausanne, Switzerland

³ Institute of Physics Academy of Sciences of the Czech Republic, Na Slovance 2, 182 21 Prague 8, Czech Republic

Received: 26 September 2003/Accepted: 24 February 2004
Published online: 26 July 2004 • © Springer-Verlag 2004

ABSTRACT Active rib waveguides with depths and widths varying from 3 to 5 μm and from 9 to 24 μm , respectively, have been structured by Ar^+ -beam etching in pulsed laser deposited Ti:sapphire layers. Losses in the channel structures were essentially at the same levels as the unstructured planar waveguide host, therefore suggesting that there is no significant additional contribution to loss from the rib-fabrication procedure. Measurements of the beam-propagation factors, M_x^2 and M_y^2 , indicate single-transverse-mode fluorescence emission. The fluorescence output power was in the order of 300 μW when the structures were pumped by a 3-W multiline argon laser. These characteristics make the rib structures suitable as light sources for optical coherence tomography applications and facilitate their coupling to the optical fibre interferometers of such systems.

PACS 42.70.Hj; 42.82.Et; 42.79.Gn; 81.15.Fg; 42.30.Wb

1 Introduction

Ti:sapphire is a particularly interesting laser material because it offers a widely tunable output (650–1100 nm) [1] and is characterized by a wide absorption band (400–650 nm). However, an adverse side-effect of this wide tunability is a low peak emission cross section, which, combined with a short fluorescence lifetime, in turn imposes as a requirement the use of high pump power densities to achieve efficient cw lasing. The undesirable prerequisite of high pump power levels can to a certain extent be overcome by adopting a planar or channel waveguide geometry. Pulsed laser deposition (PLD) has proven to be a reliable technique for the growth of waveguiding films of various laser host materials and suitable for tailoring the concentration and valence-state type of dopants in the films. This is important for the growth of Ti:sapphire layers as control of the valence state of the incorporated titanium dopant in the films can determine the waveguide laser performance [2]. To date, realization of planar waveguide lasers from PLD-grown films has so far been observed in Nd : $\text{Gd}_3\text{Ga}_5\text{O}_{12}$ [3–5] and Ti:sapphire planar guides [6]. The latter had a degree of crystal perfection and

dopant levels comparable with commercial bulk targets and the incorporated titanium was substituted for the Al^{3+} in the correct lattice position [2].

Compact fluorescence devices based on Ti:sapphire are particularly interesting for applications in biological imaging such as optical coherence tomography (OCT) due to their emission in the near infrared, which ensures an adequate penetration depth of the light in the tissue. Other attributes are the improved longitudinal resolution as a result of their large spectral bandwidth and hence short coherence length, as well as the potential for detection sensitivity and imaging of weakly backscattering structures in tissues due to their high irradiance and wide dynamic range [7, 8]. The potential of PLD-grown planar Ti:sapphire waveguides to provide spectrally broadband fluorescence with a few hundred μW of output power has already been demonstrated [9]. However, channel geometries are more promising for the development of fluorescence sources as they show better lateral confinement of both the pump and laser modes than their unstructured planar film counterparts and are capable of providing a fully diffraction-limited, near-circular, single-mode beam. Recently, two approaches have been reported towards fabrication of Ti:sapphire rib waveguides using reactive ion beam etching (RIE) [10] and Ar^+ ion beam milling [11], and both have produced structures with smooth morphological features, low propagation losses and good guiding properties.

We detail here the fabrication of Ti:sapphire rib waveguides using PLD and Ar^+ ion beam milling. Also, we report an investigation of the waveguiding behaviour of these structures in terms of their potential to have a minimum contribution to background propagation loss in the host film, as well as of their optical characteristics such as the beam-quality factor M^2 and the output power levels for fluorescence emission.

2 Fabrication methods

Depositions were performed in a stainless steel vacuum chamber, which was evacuated down to a base pressure of 5×10^{-6} mbar. Films with a thickness of $\sim 11 \mu\text{m}$ were grown on sapphire(100) substrates by pulsed laser ablation of a single-crystal Ti:sapphire target of 0.12 wt% Ti_2O_3 in a background argon atmosphere of 3×10^{-4} mbar. Ablation was performed by a KrF excimer laser (Lambda Physik, LPX 200, 248 nm, pulse duration ~ 20 ns), which was oper-

✉ Fax: +44-2380/593-142, E-mail: chg@orc.soton.ac.uk

ated at 10 Hz and focused to an energy density of $\sim 4 \text{ J/cm}^2$ on the target. Substrates were positioned at a distance of 4 cm away from the target material and were held at a temperature of $\sim 975 \text{ }^\circ\text{C}$ during growth by means of a raster-scanned 50-W CO_2 laser (Synrad 57-1-28W) [12]. This technique was preferred to other conventional heating methods as the latter would have led to overheating and desorption of impurities from the deposition chamber and therefore to contamination of the growing film. Substrate temperature is an important parameter in the deposition of Ti:sapphire layers as at temperatures below $950 \text{ }^\circ\text{C}$ no single-crystal sapphire growth can be achieved, while for settings above $1000 \text{ }^\circ\text{C}$ the concentration of the tetravalent titanium valence state progressively increases at the expense of the corresponding trivalent dopant [2, 13, 14]. The Ti^{4+} valence state is undesirable as it can lead to parasitic absorption and subsequent limitation in the device performance.

Rib waveguides were structured in the pulsed laser deposited Ti:sapphire films by photolithographic patterning and subsequent Ar^+ -beam milling. In the first step a $10\text{-}\mu\text{m}$ -thick layer of negative photoresist (SU-8, Microchem) was applied on the top of the planar waveguide and then using a chromium mask a photoresist pattern consisting of strips

with various widths was formed by standard photolithography. Subsequently, using a 500-V neutralized Ar^+ beam with an ion density of 0.9 mA/cm^2 in a background pressure of 2×10^{-6} mbar the exposed parts of the planar waveguide were etched at two different exposure angles of 40° and 0° at rates of 13 and 11 nm/min, respectively. The ribs had a trapezoidal profile and the width, d , at the top of the structure was 60% of the corresponding value w at the base for the $w = 14\text{-}\mu\text{m}$ rib. The exposure angle in the milling process has an influence on the width ratio (d/w) such that higher angles lead to more inclined side faces. After the completion of all the fabrication procedures all the photoresist remnants were removed from the top of the guide by ultrasonic cleaning in an acetone bath and the end faces of the sample were polished to an optical finish to optimize the subsequent in-coupling and out-coupling procedures. Figure 1 shows scanning electron microscope (SEM) images of Ti:sapphire ribs fabricated at an exposure angle 0° with respect to the incidence of the Ar^+ beam. The structures have a very smooth morphology, which is indicative of their potential to support low-loss guiding. We note that the face profile of the ribs had minimal influence on the fluorescence mode and 0° exposures were carried out when close spacing between the ribs was required.

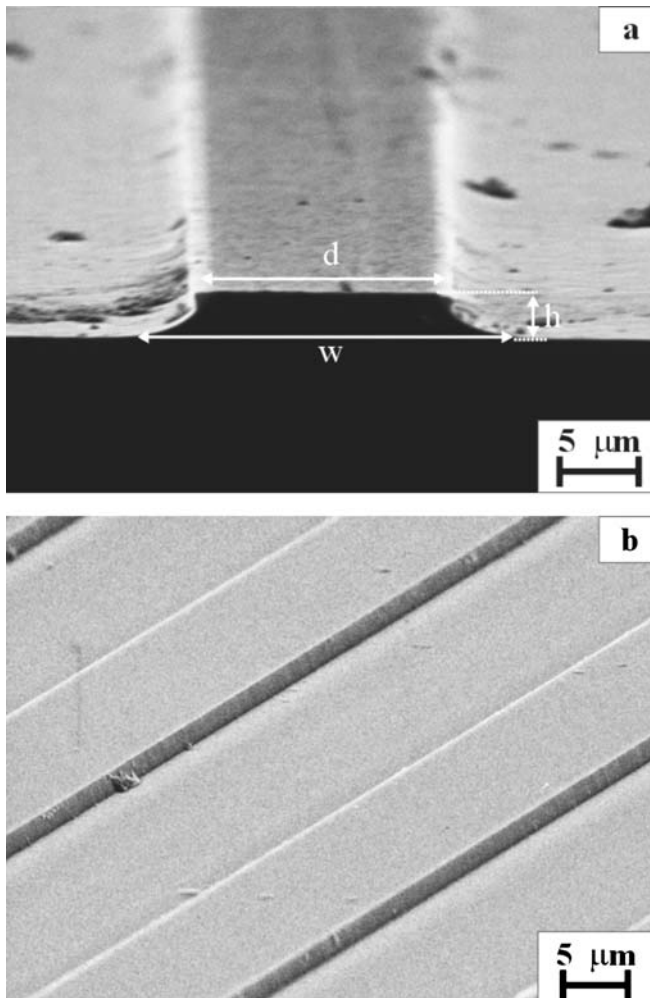


FIGURE 1 Scanning electron microscope pictures of Ar^+ -beam-structured ribs in a $10\text{-}\mu\text{m}$ -thick PLD-grown planar waveguide

3 Optical characterisation

The optical characterization of the Ti:sapphire waveguides involves (i) measurement of the propagation loss, (ii) experimental observation of the fluorescence modes as well as measurement of the fluorescence beam propagation factors and (iii) evaluation of the fluorescence output power levels with respect to the pump power. Channel waveguide structures fabricated by etching techniques usually suffer from significant scattering losses due to the roughness of the side walls. To evaluate any possible additional losses induced by the rib-fabrication process over the background level of the planar guide, which was $\sim 1.6 \text{ dB cm}^{-1}$, non-destructive propagation-loss measurements for the rib waveguides were performed via the self-pumped phase-conjugation (SPPC) method [15]. Our experimental arrangement for this has been detailed in [11]. In brief, the 720-nm output from a Ti:sapphire laser (Spectra Physics, model 3900S) was shaped to an aspect ratio of 2.5 : 1 to adequately fit that of the modes of the rib guides using a cylindrical lens telescope (two cylindrical lenses with focal lengths of $f = 25 \text{ cm}$ and 10 cm). It was then launched into the structures by a microscope objective with a magnification of $\times 6.3$. Guided light from the waveguide was coupled out with a microscope objective with a magnification of $\times 20$ and was subsequently phase conjugated via SPPC from a nominally undoped BaTiO_3 crystal using the standard total internal reflection (TIR) geometry [16]. The advantage of this technique is that the retro-reflected beam from the BaTiO_3 crystal is automatically coupled back into the waveguide without any launch losses other than the Fresnel reflections. This allows evaluation of the propagation loss through measurement of the intensity of the retro-reflected beam before and after the waveguide. This method has yielded a loss value of $1.7 \pm 0.1 \text{ dB cm}^{-1}$ for the waveguide with reproducibility within an error of 5% for a set of five measurements. Comparison between this value and the one obtained

for the Ti:sapphire planar waveguide host leads to the conclusion that the loss level remains essentially unchanged after the rib-fabrication process, which is thought to be an attribute of the very smooth features of the side walls of the rib structures.

The fluorescence characteristics were examined using an argon laser as the pump source (Coherent, model Innova 70) operating on all lines. The fluorescence emission, which was collected from the exit face of the guide, was imaged on the CCD camera after having passed through an OG 550 filter to block the residual transmitted pump irradiation. Figure 2 shows an experimentally recorded intensity fluorescence profile originating from a rib with a height h and a width w of 5 and 14 μm , respectively. The profiles indicate that the guides are suitable for producing strong optical confinement. The beam-propagation factors were measured using the knife-edge technique and showed a diffraction-limited output with values of 1.12 and 1.16 for the parallel and perpendicular directions with respect to the waveguide plane, respectively. We note that for these measurements the fluorescence emission from the guide was masked by an aperture to ensure that only the fluorescence from the rib guide itself was measured. Any contribution to the emission originating from the planar region between the ribs would have increased the M^2 value in the direction parallel to the waveguide plane via re-focusing. The strong optical confinement of the fluorescence emission, which is desirable to ensure efficient coupling to the fibre-optic interferometric arrangements used in OCT systems, indicates the potential for fabrication of closely spaced (of the order of a few tens of micrometres) multiple ribs on the same substrate.

Figure 3 shows the fluorescence output power from waveguides with two different widths, w , as a function of the input power. The maximum output powers were 283 μW ($w = 16 \mu\text{m}$) and 181 μW ($w = 10 \mu\text{m}$), and the corresponding slope efficiencies were 9.5×10^{-5} and 6.2×10^{-5} . The output power levels are in good agreement with the ones calculated [11] following a plane-wave analysis accounting for depletion of the absorbing level. To increase the fluorescence output power we have made an attempt to exploit the amplified spontaneous emission (ASE) by butt coupling a lightweight thin mirror at the in-coupling face of the waveguide using the surface tension of a small amount of fluorinated liquid. The mirror had a reflectivity of 99.8% and a transmission of 86% at the emission and pump wavelengths, respectively. This configuration leads to an increase of $\sim 46\%$

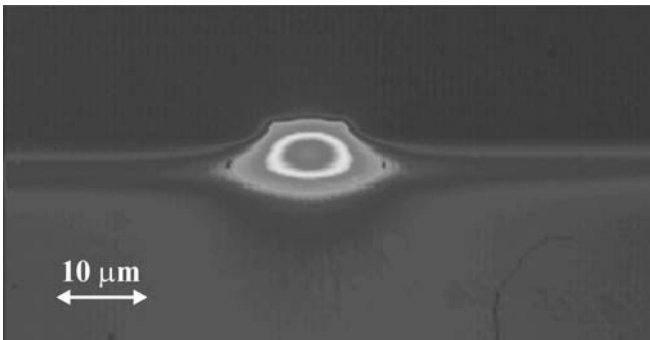


FIGURE 2 Fluorescence emission profile measured at the exit of a Ti:sapphire rib waveguide with a depth of 5 μm and a width of 14 μm

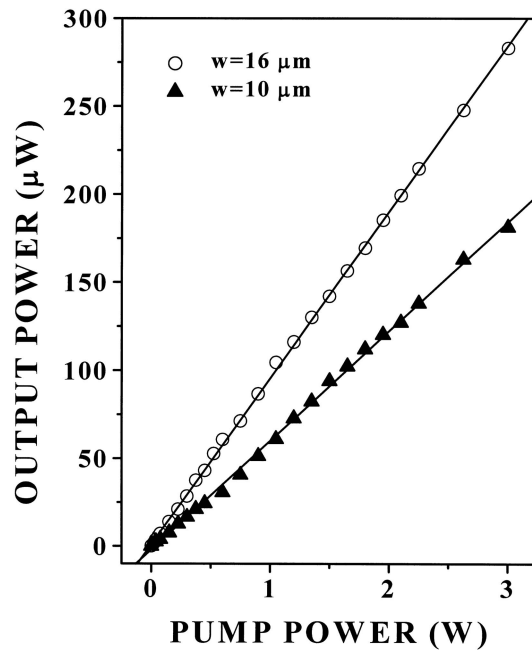


FIGURE 3 Fluorescence power as a function of pump power from an Ar^+ laser for 5- μm -deep ribs with a width value w of \circ 16 μm and \blacktriangle 10 μm

in the emitted fluorescence power, which results from the back reflection of the counter-propagating luminescence. Thus, as shown in Fig. 4, for a rib with a width w of 14 μm the maximum output power has increased from 243 to 350 μW , and the corresponding slope efficiency from 8.1×10^{-5} to 1.2×10^{-4} . The moderate increase in the output power (< 2) is likely to be due to a slight deviation of the direction of the ribs from the normal to the input and output faces of the waveguide reducing the optical feedback from the mirror. We note that a further increase in the fluorescence output can be achieved by adjusting the length of the sample to the pump absorption length.

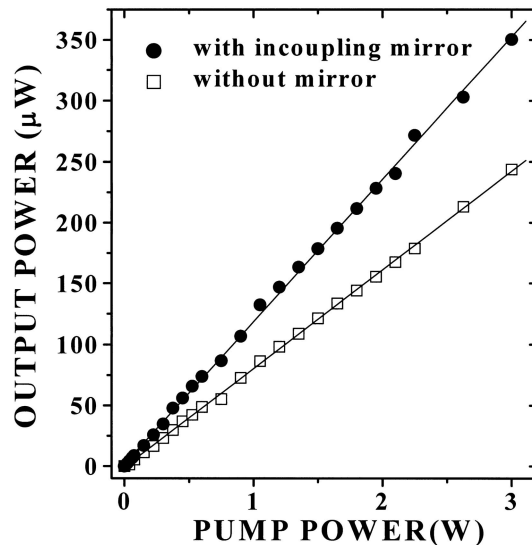


FIGURE 4 Fluorescence output as a function of pump power from an Ar^+ laser for 5- μm -deep ribs with a width value w of 14 μm with (\bullet) and without (\square) incoupling mirror

4 Conclusions

Ti:sapphire rib waveguides have been fabricated by PLD and Ar⁺-beam milling. Non-destructive loss measurements performed by the SPPC method have shown no increase in the planar waveguide background loss after the rib-fabrication procedure, which is thought to be an attribute of the very smooth morphological features of these structures as revealed by SEM studies. The rib waveguides were capable of providing fundamental mode fluorescence emission and output powers of a few hundred μW , which renders them suitable for integration with readily available OCT interferometric arrangements. Future work will be directed towards a further increase in the level of the output power that can be achieved by exploiting the effect of amplified spontaneous emission (ASE) and ultimately by demonstrating laser action. In both cases this should be achieved by minimizing the narrowing in the spectral bandwidth of the emission, as that would reduce the longitudinal resolution of the OCT interferometer. Although the current level of propagation loss in the material can support such schemes [2], it could be further reduced by applying a cladding layer on the top of the samples, which is a possibility that we are currently exploring.

ACKNOWLEDGEMENTS This research was supported by the Engineering and Physical Sciences Research Council (EPSRC) under Grant No. GR/R74154/01. One of the authors (T.C. May-Smith) wishes to acknowledge the EPSRC for a studentship.

REFERENCES

- 1 P.F. Moulton: *J. Opt. Soc. Am. B* **3**, 125 (1986)
- 2 A.A. Anderson, R.W. Eason, M. Jelinek, C. Grivas, D. Lane, K. Rodgers, L.M.B. Hickey, C. Fotakis: *Thin Solid Films* **300**, 68 (1997)
- 3 D.S. Gill, A.A. Anderson, R.W. Eason, T.J. Warburton, D.P. Shepherd: *Appl. Phys. Lett.* **69**, 10 (1996)
- 4 C.L. Bonner, A.A. Anderson, R.W. Eason, D.P. Shepherd, D.S. Gill, C. Grivas, N.A. Vainos: *Opt. Lett.* **22**, 988 (1997)
- 5 C. Grivas, T.C. May-Smith, D.P. Shepherd, R.W. Eason: *Opt. Commun.* **229**, 355 (2004)
- 6 A.A. Anderson, R.W. Eason, L.M.B. Hickey, M. Jelinek, C. Grivas, D.S. Gill, N.A. Vainos: *Opt. Lett.* **22**, 1556 (1997)
- 7 D. Huang, E.A. Swanson, C.P. Lin, J.S. Schuman, W.G. Stinson, W. Chang, M.R. Hee, T. Flotte, K. Gregory, C.A. Puliafito, J.G. Fujimoto: *Science* **254**, 1178 (1991)
- 8 J.M. Schmitt: *IEEE J. Sel. Top. Quantum Electron.* **5**, 1205 (1999)
- 9 M. Pollnau, R.P. Salathé, T. Bhutta, D.P. Shepherd, R.W. Eason: *Opt. Lett.* **26**, 283 (2001)
- 10 A. Crunteanu, M. Pollnau, G. Jänchen, C. Hibert, P. Hoffman, R.P. Salathé, R.W. Eason, C. Grivas, D.P. Shepherd: *Appl. Phys. B* **75**, 15 (2002)
- 11 C. Grivas, D.P. Shepherd, T.C. May-Smith, R.W. Eason, A. Crunteanu, M. Pollnau, M. Jelinek: *IEEE J. Quantum Electron.* **QE-39**, 501 (2003)
- 12 S.J. Barrington, R.W. Eason: *Rev. Sci. Instrum.* **71**, 4223 (2000)
- 13 P. Manoravi, P.R. Willmott, J.R. Huber, T. Greber: *Appl. Phys. A* **69**, S865 (1999)
- 14 P.R. Willmott, P. Manoravi, J.R. Huber, T. Greber, T.A. Murray, K. Holliday: *Opt. Lett.* **24**, 1581 (1999)
- 15 S. Brülisauer, D. Fluck, C. Solcia, T. Pliska, P. Günter: *Opt. Lett.* **20**, 1773 (1995)
- 16 J. Feinberg: *Opt. Lett.* **7**, 486 (1982)